Simulation and Image Reconstruction for a Low-Cost PET Detector Concept

Jemma Bagg[1], **Dr James Keaveney**[2] **and Dr Ryan Justin Atkin**[1,2]

[1]Physics, University of Cape Town, Cape Town, South Africa
[2]Physics, African Institute for Mathematical Sciences (AIMS), Cape Town, South Africa

E-mail: bggjem001@myuct.ac.za

Abstract. This project aims to develop a digital workbench through simulation to evaluate various low-cost PET detector designs. This workbench provides a fast and efficient way to reach a decision as to whether the low-cost system can produce clinically relevant images as well as determine how these designs can be optimised. The first preliminary low-cost detector design has a smaller geometry and simplified modules when compared to the commercial Philips Vereos system. Both detector models were simulated using GATE (Geant4 Application for Tomographic Emission). Data generated from the simulation is then reconstructed using a custom Maximum Likelihood Expectation Maximisation (MLEM) algorithm. The two images produced by the detectors are then compared using the Mean Squared Error (MSE) and the Structural Similarity Index Measure (SSIM), which are metrics that are able to quantify how similar the two images are. Working through this digital workbench allows for systemic evaluation of the clinical relevance of different low-cost PET designs. Future work will explore the integration of machine learning techniques to improve the image quality of the images produced by the low-cost detector design.

1 Introduction

Positron Emission Tomography (PET) is one of the most sensitive imaging techniques that is currently available in the medical world. It allows physicians to monitor metabolic activity, localise tumours and assess treatment efficiency. This is achieved by injecting patients with a radiotracer, which is absorbed by metabolically active or diseased cells, making them visible to the scanner.

It is because PET scans are so useful that the World Health Organisation (WHO) has recommended a PET scanner ratio of two scanners per million people to meet population needs [1]. In South Africa, there are currently 21 PET scanners [2], meaning nearly six times this number would be needed to align with WHO's suggested ratio, given a population of approximately 60 million people. Access to this small number of scanners is also extremely uneven. More than half of South Africa's PET scanners are located in the private healthcare sector, which serves only 18% of the population, leaving the remaining 82% with extremely limited access to this advanced imaging technology [2].

Developing a low-cost PET scanner would be a critical step towards addressing these disparities and bridging the gap in access, making advanced medical imaging more widely accessible. Beyond direct cost savings, low-cost PET systems can also reduce downstream healthcare costs, such as unnecessary tests, procedures, and prolonged treatments by enabling accurate and early diagnosis [3]. Having PET scanners more widely accessible would also help alleviate many logistical obstacles, such as reducing the travel costs that many South Africans cannot afford

when seeking the healthcare they need.

This project aims to create a digital workbench in order to evaluate the performance of low-cost PET detector designs. At the end of this workbench, an informed decision can be made as to whether the low-cost design is producing clinically relevant images. However, due to the smaller geometry and simplified modules of the low-cost design, it will almost always produce lower-quality images using conventional image reconstruction techniques when compared to the standard PET systems that already exist. This is why this project also explores the idea of enhancing the image reconstruction algorithm with machine learning (ML) in order to improve the image quality.

2 PET Imaging and Detection Principles

2.1 Physics Background

In PET imaging, patients are injected with a radiotracer that contains a positron-emitting isotope. Positron-emitting isotopes are radioactive and unstable, and so to become more stable, a proton in the nucleus transforms into a neutron through a process called beta plus (β^+) decay. This results in the emission of a positron (e^+) and an electron neutrino (ν_e), as shown in Equation 1, where Z is the proton number and A is the mass number.

$$\mathrm{M}(Z, A) \rightarrow \mathrm{M}(Z-1, A) + e^+ + \nu_e \tag{1}$$

Over time, this tracer accumulates in specific tissues in the body, depending on its biological properties. For example, the tracer will accumulate in the brain and in tumours, where glucose metabolism is high [4]. Once inside the body, the isotope decays and emits a positron, and when this positron encounters an electron in nearby tissue, they undergo an annihilation reaction. This is a fundamental process in which a particle and its antiparticle collide and their combined mass is converted into energy. The result of the annihilation reaction is the emission of two photons, each with an energy of 511 keV (the rest mass energy of the electron or positron), emitted in nearly opposite directions (approximately 180 degrees apart). These photons are detected by a ring of scintillation detectors that surround the patient.

2.2 Scintillation Detectors

When the photons produced by the positron annihilation interact with the scintillation detector, they deposit energy into the detector material. This energy causes excitation of the atoms and molecules within the scintillator. As these excited states decay back to their original state, they release the excess energy in the form of visible light photons ([5], [6]).

The amount of scintillation light produced is proportional to the energy deposited by the incident photon, making it a reliable measure of the energy of the incident photon. To convert this light into an electrical signal, PET detectors use photomultiplier tubes (PMTs) or, in modern systems, silicon photomultipliers (SiPMs) [7].

Each scintillator captures the 3D position of the interaction on the scintillator, the detection time and the energy deposited by the photon. By applying energy discrimination (keeping only events near 511 keV) and using coincidence timing, photon pairs can be identified. A straight line, known as a line of response (LOR), is drawn between the two detection points. While the LOR defines the path between two coincident detections, it only constrains the annihilation event to lie somewhere along the line; it does not indicate the exact location of the event. This positional uncertainty is why further image reconstruction algorithms are needed to reconstruct the original radiotracer distribution in the body.

2.3 Image Reconstruction

The primary task of an image reconstruction algorithm for a PET detector is to take the incomplete spatial data and transform it into an accurate image. In PET imaging, the data is mainly collected in a sinogram format. A sinogram is a convenient way to represent the measured coincidence data. It is plotted using two parameters derived from each LOR: the perpendicular distance of the LOR from the centre of the scanner (the radial distance) and the angle at which the LOR intersects the imaging plane. Each point in the sinogram thus corresponds to a specific LOR created by two coincident photon detections. The sinogram is then used as the input for many image reconstruction algorithms, which can take it and reconstruct the original distribution of radio tracer activity within the patient.

3 The Digital Workbench

3.1 Simulation Framework

The simulations in this project were performed using GATE [8], an open-source platform developed by the OpenGate collaboration. GATE builds on the Geant4 Monte Carlo toolkit [9] and provides a dedicated interface for

medical imaging simulations.

The first preliminary design is a compact PET system with simplified modules and smaller geometry, as these are both the first steps to take when trying to reduce the cost of the PET system. A module refers to an array of scintillators. This compact design is compared with a commercial Philips Vereos Digital PET system. The key differences between these two detector designs are highlighted in Table 1.

	Philips Vereos Detector	Low-Cost Detector
Radius	500 mm	160 mm
Module Dimensions	19 mm $\times$ 131.4 mm $\times$ 164 mm	15 mm $\times$ 24 mm $\times$ 24 mm
Pixels per module	1280	64

Table 1: Table showing the key differences between the low-cost, compact PET system and a commercial Philips Vereos system.

The Philips Vereos System acts as a ground truth reference for the low-cost PET system. The Philips system is known to produce images that are of a clinical standard [10], and so if the low-cost design is able to produce images of the same quality, then it has a high chance of being clinically usable. Figure 1 shows the visualisation of the two detector designs using GATE, the left image shows the low-cost PET system and the image on the right shows the commercial Philips Vereos system.

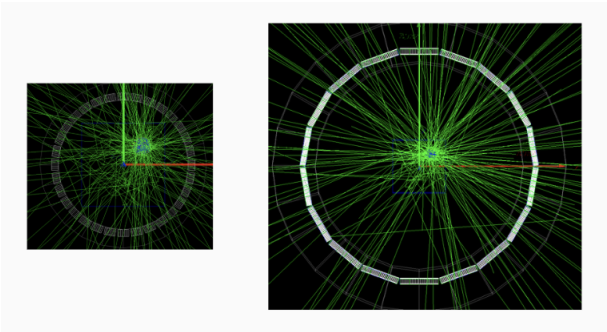

Figure 1: Visualisations of the two PET detector designs using GATE. The left image shows the low-cost system and the right image shows the commercial Philips Vereos system. The green lines represent simulated photon paths.

3.1.1 Phantoms In PET simulations, phantoms are objects that are used to mimic human tissue to validate detector performance and image reconstruction accuracy. GATE offers the flexibility to define a range of phantoms with controlled activity distributions. To simulate a realistic PET scan, a realistic brain phantom is being developed. The brain was selected as the primary focus due to the compact geometry of the low-cost detector system, which is better suited to imaging smaller regions.

The brain phantom is created by voxelising publicly available CT scan datasets into anatomically accurate regions. Voxellistion refers to the process of converting a 3D object into a grid of small volumetric units called voxels, the 3D counterpart of pixels. This is achieved by stacking the 2D slices from the CT scan to construct a 3D volume, where each voxel encodes local information, such as tissue density. Once the volume has been fully voxelised, it serves as the digital phantom input for the GATE simulation. A schematic representation of this process is shown in Figure 2.

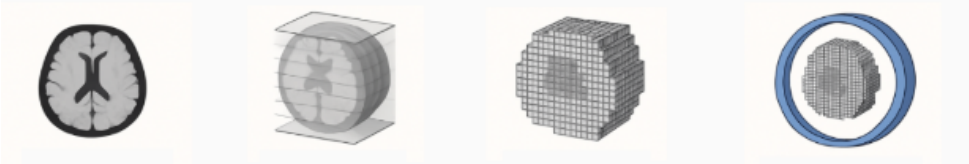

Figure 2: Process of voxelising a CT brain scan to create a digital phantom for PET simulation. From left to right: (1) a 2D CT slice of the brain, (2) stacking of multiple 2D slices to form a 3D volume, (3) conversion of the volume into a voxel grid and (4) voxelised phantom placed inside a simulated PET scanner geometry.

3.2 The Maximum Likelihood Expectation Maximisation Algorithm

The Maximum Likelihood Expectation Maximisation (MLEM) algorithm is an iterative reconstruction method widely used in PET imaging. Its objective is to estimate the spatial distribution of radiotracer activity that most likely accounts for the detected data, which is assumed to follow Poisson statistics due to the random nature of radioactive decay ([11], [12]).

The algorithm starts with an initial estimate of the radiotracer distribution (the image), which is forward-projected to generate an estimated sinogram. This simulated sinogram represents the projection data that would be observed if the current image estimate were correct.

Rather than computing a simple difference between the measured and estimated sinograms, MLEM evaluates the likelihood that the measured data D would occur given the forward projection of the image estimate $P(I)$, denoted as $L(D \mid P(I))$. A correction term is derived based on this likelihood, and it is then backprojected, updating only those voxels that contributed to each LOR.

This iterative cycle is repeated until the reconstructed image sufficiently explains the measured data. Figure 3 shows an example of reconstructed images of spherical sources using a custom implementation of the MLEM algorithm.

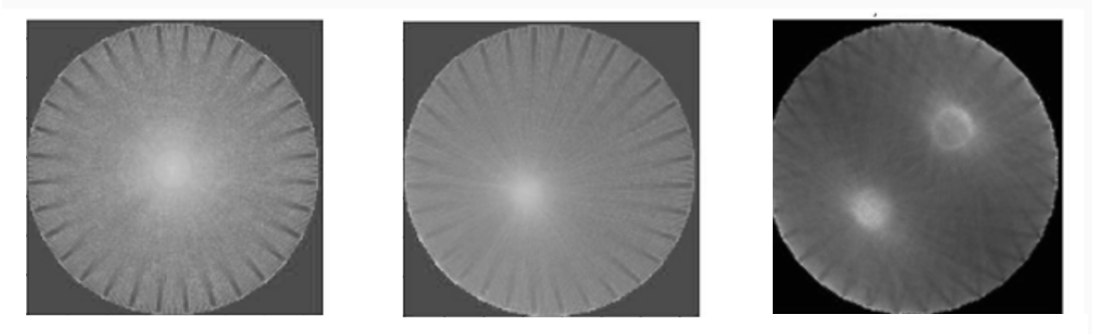

Figure 3: Reconstructed PET images using a custom MLEM algorithm. The three images show different configurations of spherical sources.

3.3 Image Comparison Metrics

Once the reconstructed images have been produced by both detector designs, a suitable metric is needed to quantify how similar the two images are. If the low-cost detector produces images that are highly similar to those generated by the commercial Philips Vereos detector, this would provide strong evidence that it may be viable for clinical use.

One of the most widely used image comparison metrics is the mean squared error (MSE), which calculates the average squared difference between corresponding pixels of two images. However, despite its simplicity, MSE is known to perform poorly in capturing perceived visual quality, particularly when structural distortions are present [13]. Studies have shown that MSE can report nearly identical values for images that appear very different to the human eye and that a large MSE doesn't necessarily mean important structural information is lost [14]. This is a

key limitation when comparing medical images, where structural information is critical.

To address this, the Structural Similarity Index Measure (SSIM) was developed as an alternative to MSE. The core idea behind the SSIM is that the human visual system is highly sensitive to structural changes, and therefore, image quality should be assessed based on the preservation of structural information ([13], [14]). SSIM evaluates the similarity between two images based on three components at each pixel: luminance (brightness), contrast and structure. In this project, SSIM is used as the main comparison metric between the low-cost and Vereos PET reconstructions. The SSIM values were computed using the structural similarity function from the scikit-image library [15]. The SSIM score ranges from -1 to 1, where a value of 1 indicates perfect structural similarity.

Figure 4 presents a comparison between the reconstructed images produced by the Philips system (left) and the low-cost PET system (right). The low-cost system yielded a MSE of 0.00493 and a SSIM of 0.6504. The relatively low SSIM score reflects the visual degradation observed, where the reconstruction from the low-cost system appears significantly noisier and contains more artefacts compared to the Philips reference.

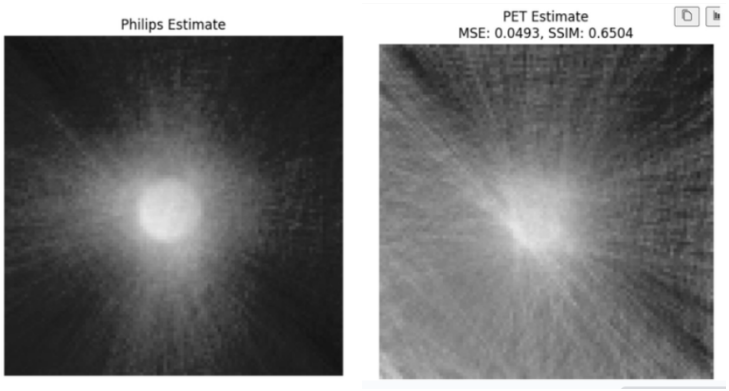

Figure 4: Comparison of reconstructed PET images from the commercial Philips Vereos system (left) and the low-cost PET system (right). The low-cost design achieved a SSIM of 0.6504 and an MSE of 0.00493.

4 Outlook

This project is still in its early stages, and one of the main challenges currently faced is the limitation in computational resources. On a standard laptop, the simulation is capable of running for only 0.1 seconds of scan time, whereas a full clinical PET scan typically lasts around 20 minutes. Scaling up to these realistic scan conditions will therefore require significant optimisation of the workflow. This becomes even more important as the anthropomorphic brain phantom is introduced, which significantly increases the complexity and volume of the data.

Figure 4 shows that the simplified modules and reduced geometry of the low-cost system lead to an inherently noisier and lower-quality image, quantified by the calculated SSIM of 0.6504. To address this, future work will focus on incorporating machine learning (ML) techniques for de-noising and reconstruction enhancement. These methods have already shown successful results in similar studies [16], and this project will make use of these results to improve the images produced by the low-cost PET system. Specifically, these studies have shown that ML can effectively restore image quality from limited or noisy data [16], addressing one of the primary challenges faced by the low-cost system. Once integrated, these ML-enhanced image reconstruction algorithms are expected to enable the low-cost system to achieve image quality comparable to that of standard PET scanners.

5 Conclusions

A fast and efficient evaluation pipeline is essential when developing low-cost PET detector systems. The ability to simulate and assess different designs allows researchers to address two key questions: Does the design produce clinically relevant images? And is the performance sufficient to serve as a viable alternative to high-cost commercial systems?

References

[1] M. Sathekge, J. M. Warwick, A. Doruyter, and M. Vorster, "Appropriate indications for positron emission tomography/computed tomography: College of nuclear physicians of the colleges of medicine of south africa," *South African Medical Journal*, 2015. [Online]. Available: https://doi.org/10.7196/SAMJ.2015.v105i11.10180

[2] A. G. Doruyter, J. Parkes, J. Carr, and J. M. Warwick, "Pet-ct in brain disorders: The south african context," *SA Journal of Radiology*, 2021. [Online]. Available: https://doi.org/10.4102/sajr.v25i1.2201

[3] A. Ellmann, "Pet/ct in south africa: a lost cause?" *SA Journal of Radiology*, 2008. [Online]. Available: https://journals.co.za/doi/10.10520/EJC100837

[4] National Research Council (US), Committee on the Mathematics and Physics of Emerging Dynamic Biomedical Imaging, *Mathematics and Physics of Emerging Biomedical Imaging*. Washington, D.C.: National Academies Press, 1996. [Online]. Available: https://www.ncbi.nlm.nih.gov/books/NBK232475/

[5] S. R. Cherry, J. A. Sorenson, and M. E. Phelps, *Physics in Nuclear Medicine*, 4th ed. Philadelphia: Elsevier Saunders, 2012.

[6] E. Moser, X. Zhang, M. Judenhofer, and S. Cherry, "Overview of pet detector technology and performance as part of the explorer total-body pet scanner project," *Physics in Medicine & Biology*, 2018.

[7] G. F. Knoll, *Radiation Detection and Measurement*, 4th ed. John Wiley & Sons, 2010.

[8] OpenGATE Collaboration, "The opengate collaboration – monte carlo simulations for medical imaging and radiotherapy," http://www.opengatecollaboration.org/.

[9] S. Agostinelli, J. Allison, K. Amako, J. Apostolakis, H. Araujo, P. Arce, M. Asai, D. Axen, S. Banerjee, G. Barrand *et al.*, "Geant4—a simulation toolkit," *Nuclear Instruments and Methods in Physics Research Section A: Accelerators, Spectrometers, Detectors and Associated Equipment*, 2003.

[10] J. van Sluis, J. R. de Jong, J. A. Schaar, R. A. Dierckx, R. J. Borra, and R. Boellaard, "Performance characteristics of the digital philips vereos pet/ct system," 2020.

[11] L. A. Shepp and Y. Vardi, "Maximum likelihood reconstruction for emission tomography," *IEEE Transactions on Medical Imaging*, 1982.

[12] K. Lange and R. Carson, "Em reconstruction algorithms for emission and transmission tomography," *Journal of Computer Assisted Tomography*, 1984.

[13] Z. Wang, A. C. Bovik, H. R. Sheikh, and E. P. Simoncelli, "Image quality assessment: From error visibility to structural similarity," *IEEE Transactions on Image Processing*, 2004. [Online]. Available: https://ieeexplore.ieee.org/document/1284395

[14] Z. Wang and A. C. Bovik, "Mean squared error: Love it or leave it? a new look at signal fidelity measures," *IEEE Signal Processing Magazine*, 2009. [Online]. Available: https://ieeexplore.ieee.org/document/4775883

[15] scikit-image developers, "Image similarity: Structural similarity index (ssim)," https://scikit-image.org/docs/0.25.x/auto_examples/transform/plot_ssim.html, 2024.

[16] F. Hashimoto, Y. Onishi, K. Ote, H. Tashima, A. J. Reader, and T. Yamaya, "Deep learning-based pet image denoising and reconstruction: a review," *Radiological Physics and Technology*, 2024. [Online]. Available: https://doi.org/10.1007/s12194-024-00780-3